Facile Production of Nanoaggregates with Tuneable Morphologies From Thermoresponsive P(DEGMA-co-HPMA)

Journal:	*Polymer Chemistry*
Manuscript ID	PY-ART-09-2015-001467.R1
Article Type:	Paper
Date Submitted by the Author:	23-Oct-2015

Complete List of Authors:	Davis, Thomas; Monash University, Monash Institute of Pharmaceutical Sciences Truong Phuoc, Nghia; Monash University, Faculty of Pharmacy and Pharmaceutical Sciences Whittaker, Michael; Monash University, Faculty of Pharmacy and Pharmaceutical Sciences; University of New South Wales, Centre Advances MAcromolecular Design Anastasaki, Athina; University of Warwick, Chemistry Department Quinn, John; Monash University, Monash Institute of Pharmaceutical Sciences Haddleton, David; University of Warwick, Chemistry Department

Facile Production of Nanoaggregates with Tuneable Morphologies From Thermoresponsive P(DEGMA-co-HPMA)

Nghia P. Truong,[a] Michael R. Whittaker,[a] Athina Anastasaki,[a,b] David M. Haddleton,[a,b] John F. Quinn*[a] and Thomas P. Davis*[a,b]

[a] *ARC Centre of Excellence in Convergent Bio-Nano Science & Technology, Monash Institute of Pharmaceutical Sciences, Monash University, Parkville, Melbourne, Victoria 3052, Australia.*

[b] *Department of Chemistry, University of Warwick, Coventry CV4 7AL, United Kingdom.*

Abstract

Thermoresponsive polymers are used to produce nanoparticles or nanoaggregates for a wide range of applications such as nanomedicine. However, low-toxicity, thermoresponsive polymers such as methacrylate polymers with short oligo(ethylene glycol) side chains are not readily applicable to the synthesis of nanoaggregates with both spherical and nonspherical morphologies. Here we report the synthesis of a low-toxicity, thermoresponsive copolymer, P(DEGMA-co-HPMA), and describe its application in the RAFT-mediated emulsion polymerization of styrene as a means to produce nanoparticles with tuneable morphology (sphere, cylinder, vesicle and lamella). These nanoaggregates offer considerable potential as a novel platform for the next generation of nanotherapeutics with improved efficacy.

Keywords: Thermoresponsive polymers, nanoaggregates, nonspherical morphology, shape of nanoparticles, toxicity, RAFT, nanomaterials, nanomedicine, and packing parameter.

Introduction

Polymeric nanoparticles or nanoaggregates hold great promise for improving diagnostic and therapeutic efficacy as well as reducing off-target accumulation and side effects.[1-3] Since the first clinical approval of nanoparticles for cancer drug delivery in 1995, a vast array of nanocarriers for both diagnostic and therapeutic applications has been engineered.[4-8] Nevertheless, despite a great deal of effort, only a handful of nanotechnology-based therapeutic products are approved for clinical use.[9-11] Due to the biological complexity and diversity of cancers and other diseases, nanocarrier platforms still need substantial improvements for the effective delivery of therapeutics with minimal side effects.[12,13] As such the reliable synthesis of biocompatible nanoaggregates with tuneable morphologies and adaptable surface chemistries is of great interest.[14-16]

Morphology or shape plays a crucial role in influencing circulation time, biodistribution, cellular uptake, intracellular trafficking and overall efficacy of nanocarriers.[17,18] In particular, nonspherical nanoaggregates such as cylinders (or "worm-like nanoparticles", (WLN)) and lamella (i.e., self-assembled polymeric membrane) exhibit longer circulation time than spherical nanoparticles.[19-21] The prolonged circulation of these nonspherical nanoparticles results in higher accumulation of therapeutics at the targeted site of diseases (e.g., larger amounts of anticancer drugs in tumor), thereby increasing drug efficacy and leading to fewer side effects.[22-24] In addition, nonspherical nanoparticles have been shown to penetrate through the cell membrane, escape from endosomal compartments, and localise in the cell nucleus.[21,25,26] On the other hand, spherical nanoparticles have exhibited an enhanced rate of cell uptake when compared to their nonspherical counterparts.[27-30] Taken together, shape of a nanoaggregate significantly impacts its pharmacokinetics and the likely utility of a nanotherapeutic formulation. Therefore, the synthesis of nanoaggregates based on low-toxicity materials with both spherical and non-spherical shape would represent a significant tool for both understanding nano-bio interactions and improving nanotherapeutic efficacy.

Thermoresponsive polymers, an important class of the so-called "smart" materials, have been widely employed as a component of amphiphilic copolymers for the synthesis of nanoparticles with various morphologies.[31-33] As a typical example, amphiphilic block copolymers incorporating poly(N-isopropyl acrylamide) (PNIPAM) with hydrophobic polystyrene (PS), or hydrophilic poly(N,N-dimethyl acrylamide) have been showed to form both spherical and non-spherical nanoaggregates.[34-39] Significantly, spherical shape has been most commonly obtained when using these amphiphilic block copolymers. To form rarer nonspherical nanoparticles in water, PNIPAM diblock copolymers have been synthesized by reversible addition fragmentation chain transfer (RAFT) polymerisation in solution or emulsion, followed by a separate self-assembly or morphological transition step.[40-42] PNIPAM is the most studied thermoresponsive polymer for the formation of nanoparticles in water. It displays a cloud point temperature (T_{cp}, the temperature at which there is a solution transition from transparent to opaque reflecting a change from soluble chains to aggregates) in water around 32 °C (i.e., below and close to human body temperature). This T_{cp} is relatively insensitive to environmental conditions.[32,43] However, PNIPAM has been shown to have appreciable toxicity and undergoes problematic interactions with proteins.[44-47] Therefore, novel classes of low-toxicity and thermoresponsive polymers are being developed as an alternative to PNIPAM for biomedical applications.[48,49]

Recently, thermoresponsive methacrylate and acrylate polymers having short oligo(ethylene glycol) side chains have been found to possess properties which are comparable with, and in some cases superior to, PNIPAM.[50-52] In particular, Lutz *et al.* have reported an interesting thermoresponsive polymer, poly(di(ethylene glycol) ethyl ether methacrylate) (PDEGMA).[53,54] PDEGMA has a lower critical solution temperature (LCST, the lowest T_{cp}) in water around 28 °C that can be tuned to 32 °C (i.e., similar to PNIPAM) by the random copolymerization of DEGMA with 5 mole percent of oligo(ethylene glycol) methacrylate.[53-56] Increasing the molar ratio of oligo(ethylene glycol) methacrylate to DEGMA leads to further increases in the LCST of these copolymers.[57] Moreover, the phase transition of PDEGMA exhibits no noticeable hysteresis (i.e., heating and cooling cycles

are roughly comparable) due to the nature of its weak intermolecular associations.[58] Importantly, PDEGMA and its copolymers are low-toxicity, antifouling, and as such have been successfully used to replace PNIPAM in a number of biomedical applications.[59-63] However, to date PDEGMA and all other thermoresponsive methacrylate polymers having short oligo(ethylene glycol) side chains have not been explored for the synthesis of biocompatible nanoaggregates with tuneable morphology.

Herein, we report the synthesis of a low-toxicity, thermoresponsive polymer based on PDEGMA, and a hydrophilic monomer *N*-(2-hydroxypropyl) methacrylamide (HPMA), P(DEGMA-co-HPMA), and its use in the RAFT-mediated emulsion polymerization of styrene to produce nanoaggregates with various morphologies in water. Five thermoresponsive P(DEGMA-co-HPMA) copolymers were synthesized by judiciously selecting the compositions and polymerization conditions. The thermoresponsive behaviour and toxicity of these novel copolymers were subsequently studied. Kinetics of the RAFT-mediated emulsion polymerization of styrene using the P(DEGMA-co-HPMA) copolymer as a macro-molecular chain transfer agent (macro-CTA) was investigated. This emulsion polymerization technique was then exploited to produce three P($DEGMA_{29}$-co-$HPMA_6$)-b-PS_z diblock copolymers suitable for the formation of nanoaggregates with various morphologies in water.

Experimental Section

Materials

Ethanethiol (97%), carbon disulfide (>99.9%), p-toluenesulfonyl chloride (>99%), thiazolyl blue tetrazolium bromide (MTT, 98%), sodium dodecyl sulfate (SDS, >99%), and dimethyl sulfoxide (>99.9%, anhydrous) were purchased from Sigma-Aldrich and used as received. Potassium hydroxide (pellet, AR grade) was obtained from ChemSupply and used as received. Di(ethylene glycol) methyl ether methacrylate (DEGMA, 95%, Sigma-Aldrich), *N*-(2-hydroxypropyl)methacrylamide (HPMA, Polysciences) and styrene (>99%, Sigma-Aldrich) were

passed through a column of basic alumina (activity I) to remove inhibitor prior to use. 4,4'-Azobis(4-cyanopentanoic acid) (ACPA, 98%, Alfa Aesar) and azobisisobutyronitrile (AIBN) were recrystallized twice in methanol prior to use. MilliQ water (resistivity > 18.2 $M\Omega cm^{-1}$) was generated using a Millipore MilliQ Academic Water Purification System. All other chemicals and solvents used were of at least analytical grade.

Synthesis of chain transfer agent (CTA), 4-cyano-4-(ethylthiocarbonothioylthio)pentanoic acid (ECT). The synthesis of ECT was carried out as previously described.[64]

Synthesis of macro-molecular chain transfer agents (macro-CTAs), P(DEGMA-co-HPMA)-SC(=S)SC$_2$H$_5$. All polymerizations were carried out in 25 mL vials equipped with a magnetic stir bar. Five macro-CTAs each incorporating a different molar percentage of HPMA (A1-A5) were synthesized by varying the initial ratio of HPMA to ECT. A typical polymerization to synthesize macro-CTA (A3) was as follows: DEGMA (1.75 g, 9.30 x 10^{-3} mol), HPMA (0.667 g, 4.65 x 10^{-3} mol), ECT (61 mg, 2.32 x 10^{-4} mol), and ACPA (5.2 mg, 1.86 x 10^{-5} mol) were dissolved in DMSO (10 mL, anhydrous). The vial was sealed with a rubber septum and the solution was deoxygenated by sparging with nitrogen for 30 min at room temperature (23 °C). After polymerizing for 7 h at 70 °C, the reaction was cooled to 0 °C by immersing the vial in an ice bath and exposed the solution to air. A 50 μL aliquot of the solution was sampled to determine conversion by ^{1}H NMR. The solution was then dialyzed against acetone (200 mL) for 1 h to remove DMSO using a dialysis membrane with molecular weight cut-off of 3.5 kDa. The polymer was recovered by precipitating into a large excess of a diethyl ether / petroleum ether mixture (2:1 v/v), after which the precipitated polymer was isolated by centrifugation and redissolved in acetone. This purification process was repeated three times. The product was dried under high vacuum for 24 h to give a sticky yellow solid (0.78 g, yield 53%).

Cell viability assay. Cell viability in presence of the macro-CTA A3 was determined using an MTT assay. HT1080 fibrosarcoma cells were seeded onto a 96-well plate at an initial density of 5 x 10^3

cells per well in 100 μL of DMEM containing 10% FBS and were then incubated at 37 °C and 5% CO_2 for 24 h. The macro-CTA A3 was dissolved in DMEM containing 10% FBS by vortexing for 10 min. The medium in each well was removed and replenished with 100 μL of fresh DMEM medium containing 10% FBS along with different concentrations of the macro-CTA A3. The plates were then incubated for 48 h at 37 °C and 5% CO_2. The cells were then rinsed with 100 μL of fresh medium, followed by the addition of 10 μL of MTT solution (5 mg/mL). The purple crystals were allowed to form for a further 4 h at 37 °C, after which 100 μL of DMSO was added to dissolve the crystals. The absorbance at 570 nm was measured for each well using a microplate reader. The experiments were performed in triplicate, and relative cell viability was calculated as the percentage viable compared to control cells in DMEM medium containing only 10% FBS (i.e., without the addition of macro-CTA A3).

RAFT-mediated emulsion polymerization of styrene in water at 70 °C using P(DEGMA$_{29}$-co-HPMA$_6$)-SC(=S)SC$_2$H$_5$ as macro-CTA. All emulsion polymerizations were carried out in 10 mL Schlenk tubes equipped with a magnetic stirrer. Different chain lengths of polystyrene block were synthesized by changing the ratio of styrene to the macro-CTA A3 (i.e., 30, 60, and 90 to 1). A typical polymerization was as follows: Macro-CTA A3 (100 mg, 1.50 x 10^{-5} mol), and SDS (2.0 mg, 7.0 x 10^{-6} mol) were dissolved in MilliQ water (4 mL) in a Schlenk tube. The tube was sealed with a rubber septum and the solution was deoxygenated by sparging with nitrogen for 25 min at ambient temperature, and then heated to 70 °C for 5 min to form a latex under a nitrogen atmosphere. AIBN (1.0 mg, 6.0 x 10^{-6} mol) was dissolved in styrene (0.4 mL) in a 1.5-mL vial. The vial was sealed with a rubber septum and the solution was deoxygenated by sparging with nitrogen for 10 min at room temperature prior to use. After 30 min, a portion of the deoxygenated styrene (0.1 mL, 9.0 x 10^{-4} mol) was added into the Schlenk tube using a gas-tight syringe to start the polymerization. After 4 h stirring at 70 °C and 700 rpm, the emulsion polymerization was stopped by exposing the latex to air at 70 °C. For the kinetic study, approximately 0.1 mL of the emulsion was sampled periodically during the polymerization using a gas-tight syringe. These samples were

used to evaluate conversion (by ^{1}H NMR), and molecular weight (by SEC) as a function of reaction time.

Formation of nanoparticles with different morphologies from hot latexes after the RAFT-mediated emulsion polymerization of styrene. 0.5 mL aliquots of hot latex from the Schlenk tube were transferred to 1.5-mL vials each having a different amount of toluene (i.e., 10 μL, 20 μL, 40 μL, 80 μL). These vials were sealed, vortexed for 2 seconds, and then slowly cooled to room temperature (23 °C) over 24 h by leaving these vials sit on the bench. To remove residual styrene and the toluene and SDS additives, the latex was dialyzed against water (100 mL x 8) for 72 h using a dialysis membrane with molecular weight cut-off of 12 kDa. To cut long WLN into short WLN by ultrasound, the WLN solution was cooled to 0 °C in an ice bath, and cut into short nanorods using an ultrasound probe (1.6 mm microtip, Q125, Qsonica) with a pulse sequence of 15 seconds on and 15 seconds off at 30% amplitude for a total of 5 min.

Characterization Techniques

^{1}H Nuclear Magnetic Resonance (NMR). All NMR spectra were recorded on a Bruker Advance III 400 MHz spectrometer using an external lock and referenced to the residual nondeuterated solvent. A mixture of deuterated acetone and deuterated chloroform (5:5 v/v) was used in the analysis of conversion of the emulsion polymerizations by ^{1}H NMR.

Size Exclusion Chromatography (SEC). SEC analyses of polymer samples were performed using a Shimadzu modular system comprising a DGU-12A degasser, an SIL-20AD automatic injector, a 5.0 μm bead-size guard column (50 × 7.8 mm) followed by three KF-805L columns (300 × 8 mm, bead size: 10 μm, pore size maximum: 5000 Å), a SPD-20A ultraviolet detector, and an RID-10A differential refractive-index detector. The temperature of columns was maintained at 40 °C using a CTO-20A oven. The eluent was *N,N*-dimethylacetamide (HPLC grade, with 0.03% w/v LiBr) and the flow rate was kept at 1 mL/min using a LC-20AD pump. A molecular weight calibration curve

was produced using commercial narrow molecular weight distribution polystyrene standards with molecular weights ranging from 500 to 2 x 10^6 g mol^{-1}. Polymer solutions at approx. 2 mg mL^{-1} were prepared and filtered through 0.45 μm filters prior to injection.

Dynamic Light Scattering (DLS). Cloud point temperature (T_{cp}) was identified by a sudden change in particle size using DLS.[65-67] Dynamic light scattering measurements were performed using a Malvern Zetasizer Nano Series running DLS software and operating a 4 mW He-Ne laser at 633 nm. Analysis was performed at an angle of 173° and a constant temperature of 25 °C. The sample refractive index (RI) was set at 1.59 for polystyrene. The dispersant viscosity and RI were set to 0.89 $Ns.m^{-2}$ and 1.33, respectively. Macro-CTAs (A1 to A5, 10 mg) were dissolved in cold MilliQ-water (1 mL) by vortexing for 10 min. The measurements were carried out by slowly increasing the temperature from 15°C to 60 °C using Standard Operating Procedures function of the DLS software. The samples were incubated for 5 min at each temperature prior to measurement.

Transmission Electron Microscopy (TEM). TEM images were recorded without staining using a Tecnai F20 or Tecnai F30 transmission electron microscope at an accelerating voltage of 200 kV at ambient temperature. A typical TEM grid preparation was conducted as follow: a 2 μL aliquot of a 0.1 wt% solution was dropped onto a Formvar-film copper grid (GSCu100F-50, Proscitech), after which samples were allowed to dry under air.

Results and discussion

Synthesis of thermoresponsive macro-CTAs. A series of five P(DEGMA-co-HPMA)-$SC(=S)SC_2H_5$ copolymers with different proportions of HPMA (A1-A5) were synthesized by RAFT-mediated solution polymerization in anhydrous DMSO for 7 h at 70 °C (see Table 1 and Scheme 1A). PDEGMA was chosen as the main component of this novel series due to its aforementioned excellent thermoresponsive, antifouling properties and biocompatibility. The hydrophilic component used for tuning the T_{cp} of these thermoresponsive copolymers was HPMA because the biocompatibility of PHPMA has been clinically tested; and the pendant hydroxyl

functionality group can be used for subsequent bioconjugation.[68-70] ECT was selected as CTA for the synthesis of these copolymers for a number of reasons: it has high stability in water, it is suitable for controlling the RAFT polymerization of a wide range of monomers (e.g., methacrylates, styrenics, etc.), and it possesses a relatively low-toxicity trithiocarbonate end group.[31,71,72] In addition, using a CTA with a trithiocarbonate functional group in the RAFT-mediated polymerization of HPMA led to higher conversion (43%) compared to using a CTA with a dithiobenzoate (6%), under otherwise identical conditions.[73] It is worth noting that all three components of the novel polymers are well tolerated and commercially available. Table 1 shows the feed ratios and characterization of all five macro-CTAs. The relatively low dispersities ($Đ$ < 1.2), and the symmetrical, unimodal molecular weight distributions (MWDs, see Fig. 1A) of all copolymers synthesized indicates the "controlled" characteristics expected under the RAFT mechanism. The number-average molecular weights (M_n) obtained using SEC were higher than those expected from theoretical calculations because of differences in the hydrodynamic volume of the polystyrene standards used for SEC calibration and that of the macro-CTAs.[64] The molar percentages of HPMA units in the copolymers were varied from 0% to 34% by simply changing the feed ratios of HPMA to ECT. The presence of HPMA units in the copolymer and the molar ratio to DEGMA was further confirmed by ^{1}H NMR (see Fig. 1B). These five copolymers incorporating different molar percentages of HPMA were used to establish the relationship between the hydrophilic repeating unit content and the T_{cp} of the copolymers. In short, five well-defined copolymers were successfully synthesized by carefully selecting both components and polymerization conditions.

Table 1. SEC and ^{1}H NMR data for the RAFT polymerization of DEGMA and HPMA with different molar percentage of HPMA (A1-A5) at 70 °C in DMSO for 7 h using ACPA as initiator.

Macro -CTA	[DEGMA]:[HPMA] :[ECT]:[I]	SEC[a]		^{1}H NMR					
		M_n (g/mol)	$Đ$	Conversion (%)		Repeating unit (n)		% HPMA[f]	$M_{n,theory}$[g] (g/mol)
				DEGMA[b]	HPMA[c]	DEGMA[d]	HPMA[e]		
A1	480:480:12:1	11,200	1.15	83	43	33	17	34	8,898
A2	480:360:12:1	10,000	1.14	87	47	35	14	29	8,845
A3	480:240:12:1	8,800	1.16	72	32	29	6	17	6,573
A4	480:120:12:1	8,400	1.18	72	30	29	3	9	6,144
A5	480:0:12:1	8,100	1.16	78	0	31	0	0	6,091

[a] SEC data measured in DMAc + 0.03 wt% of LiBr solution and using PS standards for calibration. [b] Conversions of DEGMA were calculated by the integral area of a peak at 6.0 ppm ($I_{6.0}$) and a peak in the range 3.9-4.2 ($I_{3.9\text{-}4.2}$) using the following equation: Conversion of DEGMA = 100 x 2 x $I_{6.0}$ / $I_{3.9\text{-}4.2}$. [c] Conversions of HPMA were calculated by the integral area of a peak at 5.3 ppm ($I_{5.3}$) and a peak in the range 4.6-4.7 ($I_{4.6\text{-}4.7}$) using the following equation: Conversion of HEAA = 100 x $I_{5.3}$ / $I_{4.6\text{-}4.7}$. [d] Repeating units of DEGMA were calculated using the following equation: n = conversion / 100 x [DEGMA] / [ECT]. [e] Repeating units of HPMA were calculated using the following equation: n = conversion /100 x [HPMA] / [ECT]. [f] % HPMA were calculated using the following equation: % HPMA = 100 x n_{HPMA} / (n_{DEGMA} + n_{HPMA}). [g] $M_{n,theory}$ were calculated using the following equation: $M_{n,theory}$ = n_{DEGMA} x 188 + n_{HPMA} x 143 + 263.

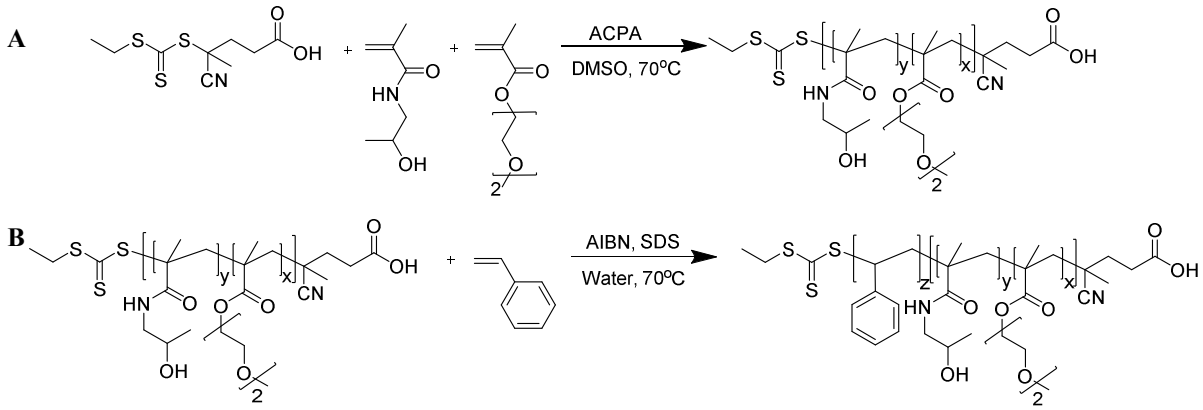

Scheme 1. (A) Synthesis of P(DEGMA-co-HPMA)-SC(=S)SC_2H_5 macro-CTAs. (B) RAFT-mediated emulsion polymerization of styrene in water.

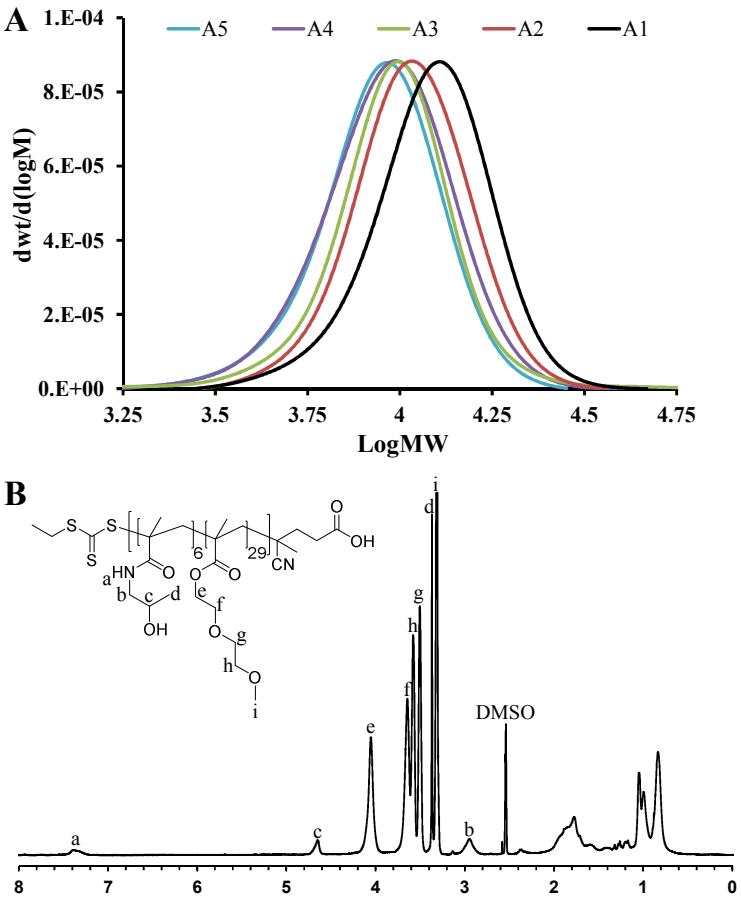

Figure 1. (A) MWDs of P(DEGMA-co-HPMA)-SC(=S)SC_2H_5 macro-CTAs with different molar ratios of HPMA (A1-A5) polymerized at 70 °C in DMSO for 7 h. (B) ^{1}H NMR of macro-CTA A3 in DMSO-d_6.

Cloud point temperature and in vitro toxicity of thermoresponsive copolymers. The well-defined P(DEGMA-co-HPMA)-SC(=S)SC_2H_5 copolymers were then examined for thermoresponsive behaviour and *in vitro* toxicity. Firstly, the T_{cp} for these copolymers was determined by identifying a sudden change in particle size using Dynamic Light Scattering (DLS).[65-67] Interestingly, the T_{cp} linearly increased with the increasing content of HPMA which could be explained by the enhanced hydrophilicity of its copolymers (see Fig. 2A). The ether oxygens in the di(ethylene glycol) units form stabilizing H-bonds with water which compete with the hydrophobic effect of the carbon-carbon backbone.[50,58,74,75] This competition creates a hydrophobic-hydrophilic balance (or

amphiphilicity) and thermoresponsive behavior of PDEGMA. The incorporation of the hydrophilic HPMA component to PDEGMA increases the mixing enthalpy of its copolymer and shifts the balance to more hydrophilic.[76,77] Thus, a higher temperature is needed to increase the Gibbs free energy of mixing to a positive value ($\Delta G_{mixing} > 0$) and to change the solution behaviour of the copolymer from water-soluble chains to aggregates.[76,78] The linear relationship between T_{cp} and the hydrophilic component provides a useful handle for generating thermoresponsive P(DEGMA-co-HPMA)-SC(=S)SC_2H_5 copolymers with tunable T_{cp}. Further, the T_{cp} of these copolymers can be easily predicted using equation 1.

$$T_{cp} = 28 + 0.7 \text{ x } \%\text{HPMA } (°C) \quad (1)$$

where %HPMA is the molar percentage of HPMA in the copolymer; and T_{cp} is the cloud point temperature of P(DEGMA-co-HPMA)-SC(=S)SC_2H_5 copolymer at specific molar percentage of HPMA.

The aim of this work is to use the thermoresponsive P(DEGMA-co-HPMA)-SC(=S)SC_2H_5 as a hydrophilic component or corona of nanoparticles at 37 °C (i.e., human body temperature). Therefore, the macro-CTA A3 having T_{cp} of 40 °C was chosen for all further studies. In the next phase of work, the *in vitro* cytotoxicity of the copolymer A3 was evaluated over a wide range of concentration (from 1 µg/mL to 10 mg/mL) using an MTT assay. Although all three components of the copolymer are well-tolerated, it is still necessary to confirm the low toxicity of the copolymer, especially at a very high concentration of 10 mg/mL. Figure 2B shows that the P($DEGMA_{29}$-co-$HPMA_6$)-SC(=S)SC_2H_5 is well-tolerated across the range of tested concentrations. The cell viability remained close to 100% compared to the control (without added copolymer), and only reduced to about 80% at the extreme concentration of 10 mg/mL. The morphology of cells at this highest concentration remained similar to that of the control (data not shown). In short, the

thermoresponsive macro-CTA A3 is a very promising candidate for the synthesis of biocompatible nanoaggregates with tunable morphologies.

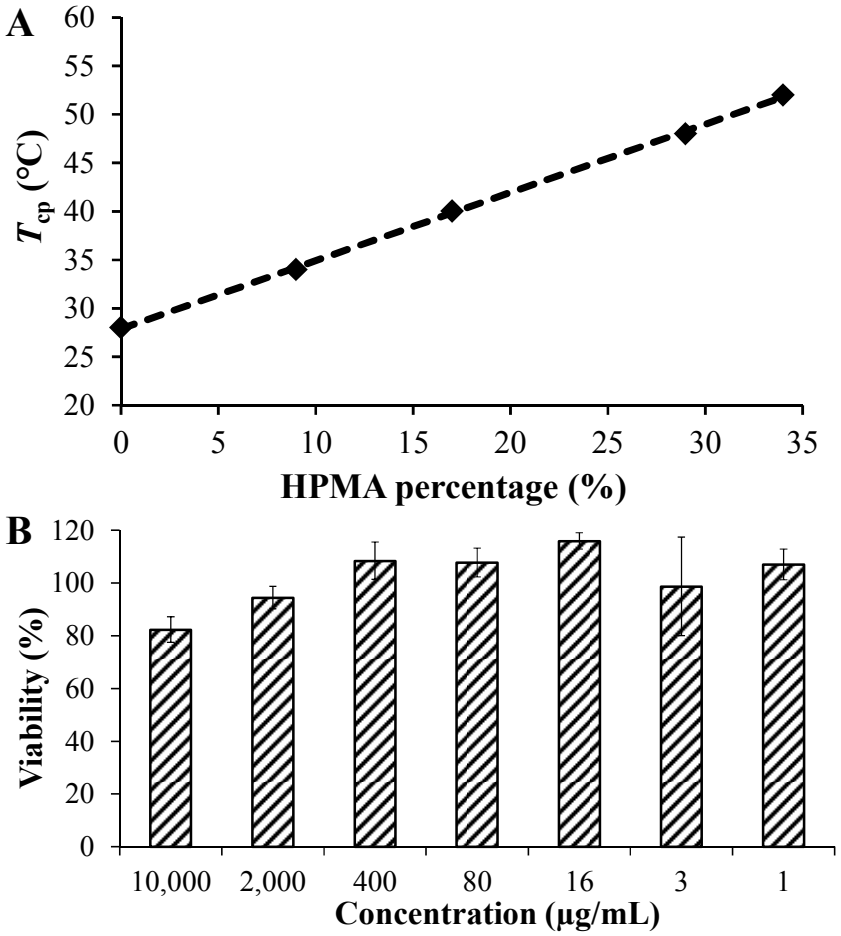

Figure 2. (A) Cloud point temperature (T_{cp}) of P(DEGMA-co-HPMA)-SC(=S)SC_2H_5 macro-CTAs incorporating different molar percentages of HPMA (A1-A5). (B) Relative cell viability values for HT1080 cells evaluated by MTT assay after incubation with the macro-CTA A3 at various concentrations for 48 h.

Kinetic study of RAFT-mediated emulsion polymerizations of styrene using thermoresponsive macro-CTA A3. To test whether P($DEGMA_{29}$-co-$HPMA_6$)-SC(=S)SC_2H_5 can be used as a macro-CTA for the RAFT-mediated emulsion polymerization of styrene, the kinetics of this polymerization were first studied. It is important to note that we chose emulsion polymerization as a

technique to synthesize the diblock copolymers with PS because of the following advantages: (i) the polymerization is fast, (ii) the reaction proceeds to high conversion, (iii) there are minimal side reactions, (iv) there is no use of organic solvents, and (v) the final product is a nanoparticle.[64] In addition, PS is selected as the hydrophobic component in this work for the following reasons: (i) the phenyl rings of PS provide high contrast in TEM characterization; (ii) the glassy styrenic cores ensure that the morphologies of nanoaggregates are stable in both solution and dry state;[16,42] and (iii) nanoparticles with stable styrenic cores have previously been used for *in vivo* drug delivery applications.[19,22] To conduct the emulsion polymerization (see Scheme 1B), the macro-CTA A3 was first dissolved in MilliQ water with a small amount of added SDS. The concentration of SDS was 1.75 mM, well below its critical micelle concentration (8 mM); and hence, SDS could not self-assembly into micelles.[79] After 25 min sparging with nitrogen, the solution of macro-CTA A3 was heated to 70 °C to form nanoaggregates stabilized by SDS.[80-82] The latex was then stirred at 70 °C for 5 min to ensure the majority of the macro-CTA chains self-assembled into nanoaggregates before styrene was added to commence the emulsion polymerization. Noteworthy, deoxygenating styrene in a separate vial ensured the precise amount of styrene at the start of the polymerization.[64] Table S1 and Figure 3 summarize the polymerization kinetics, as characterized by ^{1}H NMR, and SEC. The reaction was nearly complete (i.e., conversion reached 95%) after only 4 h (see Fig. 3A). The accelerated rate of this reaction is a typical feature of emulsion polymerization due to compartmentalization or confined space effect.[64] The excellent agreement between the M_n determined by SEC and that predicted from theory (see Table S1), and the linear increase in M_n with conversion (see Fig. 3B) indicate the well-controlled character of the emulsion polymerization under the RAFT mechanism. In addition, the MWDs shift to higher molecular weight with increasing conversion, confirming a good "controlled" RAFT polymerization and successful chain extension (see Fig. 3C). A small, high molecular weight shoulder appeared in the MWD after 3 h and 4 h, which is likely caused by bimolecular coupling at very high conversion. That said, the dispersities still remain relatively low ($Đ \leq 1.21$), which is very important for reproducibly yielding

uniform morphologies.[16,83] Altogether, these results suggest that P(DEGMA$_{29}$-co-HPMA$_6$)-SC(=S)SC$_2$H$_5$ is a suitable macro-CTA for the synthesis of thermoresponsive polystyrene diblock copolymers via RAFT-mediated emulsion polymerization.

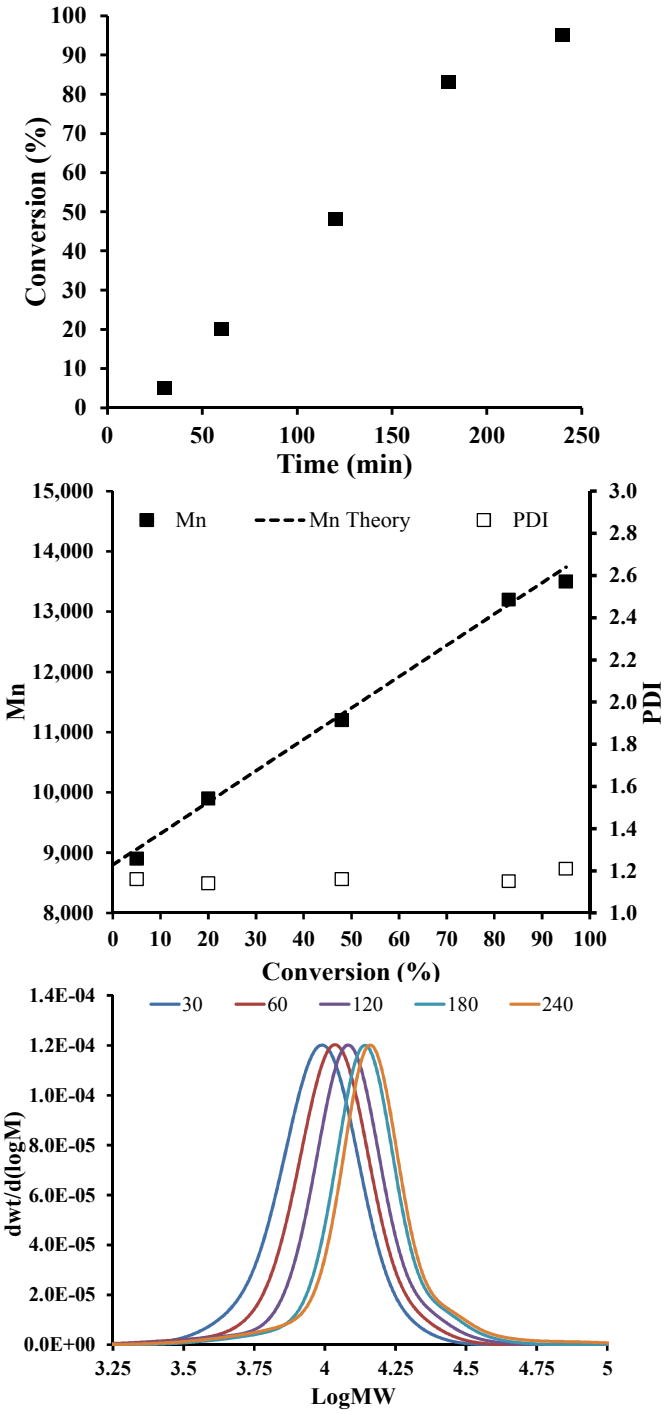

Figure 3. (A) Kinetics plot, (B) molecular weight evolution, and (C) MWDs for the RAFT-mediated emulsion polymerization of styrene in water at 70 °C using P($DEGMA_{29}$-co-$HPMA_6$)-$SC(=S)SC_2H_5$ (A3) as macro-CTA and AIBN as initiator.

Synthesis of polystyrene diblock copolymers and formation of nanoaggregates with various morphologies in water. Having confirmed that the thermoresponsive copolymer A3 is low-toxicity and suitable for the RAFT-mediated emulsion polymerization of styrene, P($DEGMA_{29}$-co-$HPMA_6$)-b-PS_z diblock copolymers were synthesized and applied for the formation of nanoparticles having different morphologies (see Table 2). By appropriate variation of the ratio of styrene to macro-CTA, three different molecular weight PS blocks (B1, B2, B3) were obtained after 3.5 h, 4 h, 4.5 h, respectively. The polymerization time from B3 to B1 was reduced to minimize bimolecular coupling at very high conversions (> 93%). Importantly, the high conversion is essential to reproducibly produce nanoparticles with uniform morphologies because the presence of excess styrene affects the formed morphologies. All three well-defined diblock copolymers have relatively low dispersities and excellent agreement between the M_n determined by SEC and that calculated from ^{1}H NMR (see Table 2). The presence of phenyl ring protons in a typical ^{1}H NMR of B3 (see Fig. S1) and the shift in the MWDs to higher molecular weights (see Fig. S2) confirm the success of all three emulsion polymerizations. It is worthwhile to note that when using deuterated chloroform for the ^{1}H NMR of the diblock copolymers, all protons of the HPMA units do not appear in these spectra due to low solubility of HPMA moieties in this solvent. As such, the repeating units of styrene are calculated without the interference of overlapping peaks from HPMA. These repeating unit values are further confirmed by those values estimated from SEC (see Table 2).

After successfully obtaining three P($DEGMA_{29}$-co-$HPMA_6$)-b-PS_z diblock copolymers as hot milky solutions (70 °C), these latexes were slowly cooled to room temperature (23 °C, below the T_{cp} of thermoresponsive copolymer A3) with or without added toluene. When cooling from 70 °C to room temperature, the thermoresponsive block A3 changes in amphiphilicity (from hydrophobic to hydrophilic, or aggregated to water-soluble), and hence drives the restructuring of the diblock

copolymer assemblies to different morphologies (see Scheme 2).[39-41] For example, Figure 4 shows the restructuring from spherical nanoaggregates (with no added toluene) to long WLN (with 20 and 40 μL/mL of added toluene), a mixture of WLN and vesicles (with 80 μL/mL of added toluene), and vesicles (with 160 μL/mL of added toluene). The morphology of spherical nanoaggregates with no added toluene is similar to that at 70 °C (see Figure S3). While spherre (at 70 °C or with no added toluene) is the typical shape of nanoaggregates with a DEGMA component, WLN is a rare morphology that can only be observed in the presence of a plasticizer.[84] Toluene was chosen as the plasticizer to tune the morphology of P($DEGMA_{29}$-co-$HPMA_6$)-b-PS_z copolymers due to its suitable solubility parameter (δ). The PS cores and toluene have very similar solubility parameters (i.e., δ_{PS} = 16.6−20.2, and $\delta_{toluene}$ = 18.2) leading to a large proportion of the added toluene being sequestered in the PS cores and the increasing in the volume of hydrophobic chains (υ).[85-87] Equation 2 describes the packing parameter (*p*) which is widely used for the prediction and explanation of diblock copolymer morphology.[88,89]

$$p = \upsilon/al \qquad (2)$$

where *p* is the packing parameter; υ is volume of hydrophobic chains; a is effective interfacial area at the hydrophobic-water interface; and *l* is the length of hydrophobic chains.

From this equation, an increase of υ leads to a higher value of *p* and the morphological transition from cylindrical to vesicle (see Fig. 4).[90,91] A similar trend of temperature-induced morphological transformation (i.e., cylindrical to lamella) was also observed for nanoaggregates derived from B1 (see Fig. S4). Interestingly, the morphological transition of nanoaggregates derived from B3 is different to that for those using B1 and B2. Figure 5 shows the transformation from large spheres (diameter ~ 1.3 μm, with no added toluene) to small spheres (diameter ~ 15 nm, with 20 and 40

μL/mL of added toluene), a mixture of small spheres and short WLN (with 80 μL/mL of added toluene), and long WLN (with 160 μL/mL of added toluene). While the transition from spherical (with 20 and 40 μL/mL of added toluene) to cylindrical morphology (with 160 μL/mL of added toluene) with increasing toluene is still associated with increasing of υ and *p* for B3, the shapes of nanoaggregates derived from B3 were different to those from B1 and B2 because of B3's longer hydrophobic chain length (*l*). For the same amount of added toluene (e.g., 40 μL/mL or 160 μL/mL), B3 has higher *l* and lower *p* than B1 and B2. Thus, the value of *p* for B3 shifts from ~ 1/3 (sphere) to ~ 1/2 (cylinder) while the value of *p* for B1 and B2 changes from ~ 1/2 (cylinder) to ~ 1 (vesicle or lamella).[90] It should be noted that at the concentration of 160 μL/mL, a very thin layer of toluene is observed on the top of all latexes (B1 to B3) indicating that nanoparticle cores are effectively saturated with added toluene.

Additionally, long WLN were successfully cut to short WLN using ultrasound, a technique first reported by Winnik et al (see Fig. S5).[92] These short WLN may be more useful for drug and gene delivery applications.[16,26] Further, all morphologies produced from copolymers B1-B3 were retained under dialysis for three days in water to remove impurities (i.e., toluene and SDS, see Fig. S6 and S7). The excellent stability of these morphologies at room temperature is attributed to the glassy PS cores (T_g ~ 100 °C).[93] Interestingly, the latex of long WLN after dialysis was able to form a free-standing physical hydrogel when heated to 50 °C (i.e., above the T_{cp} of A3), which is the typical and useful property of long WLN (see Fig. S8).[94] The morphology of long WLN is also retained at 50 °C (see Figure S9). In summary, by manipulating the volume (υ) and length (*l*) of hydrophobic chains (through adding a plasticizer and controlling the degree of polymerization), nanoaggregates with different morphologies were synthesized in water via the RAFT-mediated emulsion polymerization and subsequent temperature-induced morphological transformation using a low-toxicity, thermoresponsive P($DEGMA_{29}$-co-$HPMA_6$)-$SC(=S)SC_2H_5$.

Table 2. ^{1}H NMR and SEC data of the RAFT-mediated emulsion polymerization of styrene in water at 70 °C using AIBN as initiator and A3 as a macro-CTA.

Copolymer	[Styrene]:[Macro-CTA]:[I]	Time (h)	^{1}H NMR			SEC[d]		
			Conv[a] (%)	$N_{STY,NMR}$[b]	$M_{n,theory}$[c] (g mol^{-1})	$M_{n,SEC}$ (g mol^{-1})	$N_{STY,SEC}$[e]	$Đ$
B1	30:10:1	3.5	93	24	11,317	11,300	24	1.19
B2	60:10:1	4.0	98	55	14,478	14,200	52	1.20
B3	90:10:1	4.5	97	78	16,954	17,100	80	1.25

[a] Conversions of styrene were calculated by the integral area of a peak at 5.7 ppm ($I_{5.7}$) and a peak in the range 6.3-7.5 ($I_{6.3\text{-}7.3}$) using the following equation: Conversion of styrene = 100 x 5 x $I_{5.7}$ / $I_{6.3\text{-}7.3}$. [b] Repeating units of styrene calculated from ^{1}H NMR of purified product ($N_{STY,NMR}$) were calculated by a peak in the range 3.5-3.8 ($I_{3.5\text{-}3.8}$) and a peak in the range 6.3-7.3 ($I_{6.3\text{-}7.3}$) using the following equation: $N_{STY,NMR}$ = $I_{6.3\text{-}7.3}$ / $I_{3.5\text{-}3.8}$ x 174 / 5. [c] $M_{n,theory}$ were calculated using the following equation: $M_{n,theory}$ = 104 x $N_{STY,NMR}$ + 8,800. [d] SEC data measured in DMAc + 0.03 wt% of LiBr solution and using PS standards for calibration. [e] Repeating units of styrene calculated from SEC ($N_{STY,SEC}$) were calculated using the following equation: $N_{STY,SEC}$ = ($M_{n,SEC}$ – 8,800) / 104.

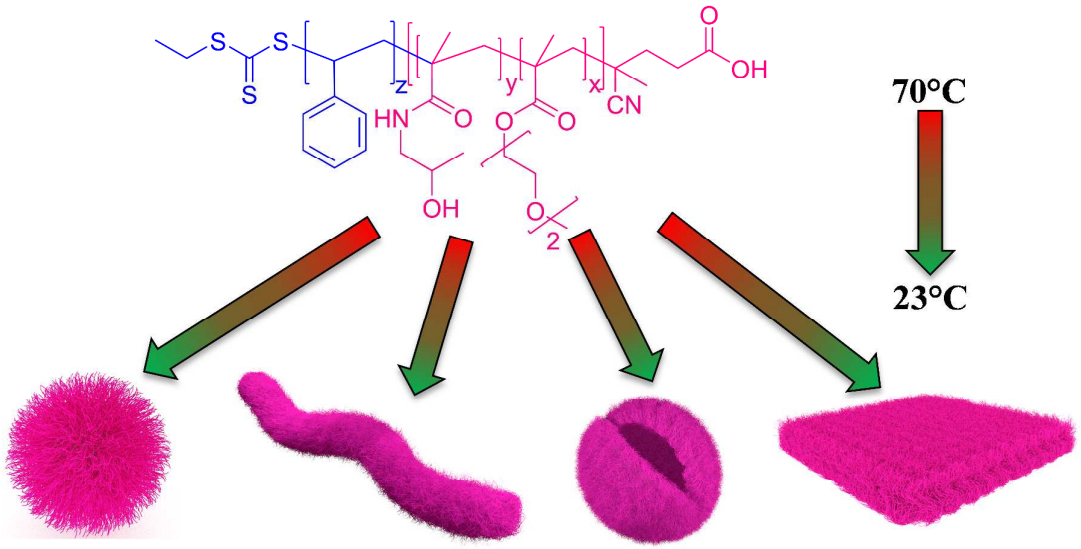

Scheme 2. Production of nanoaggregates with different morphologies in water from thermoresponsive and low-toxicity P(DEGMA$_{29}$-co-HPMA$_{6}$) by RAFT-mediated emulsion polymerization of styrene, followed by temperature-induced morphological transformation.

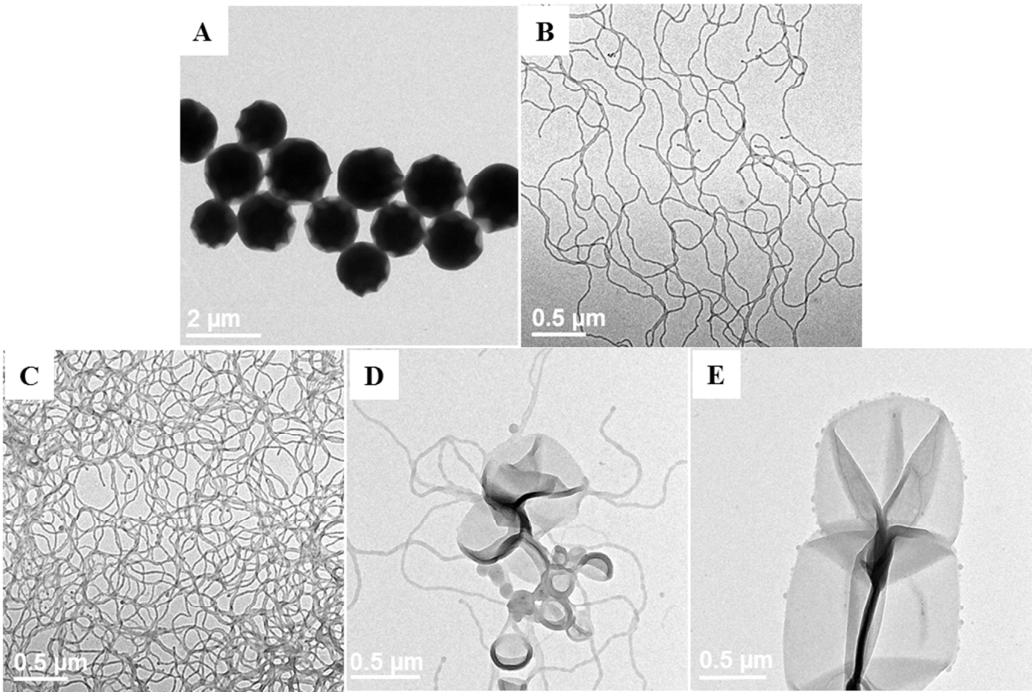

Figure 4. Representative TEM images of the latexes of diblock copolymer B2 in water after 4 h of polymerization, and after adding different amounts of toluene (A) 0 µL/mL, (B) 20 µL/mL, (C) 40 µL/mL, (D) 80 µL/mL, (E) 160 µL/mL, and then cooling to room temperature (23 ° C) for 24 h.

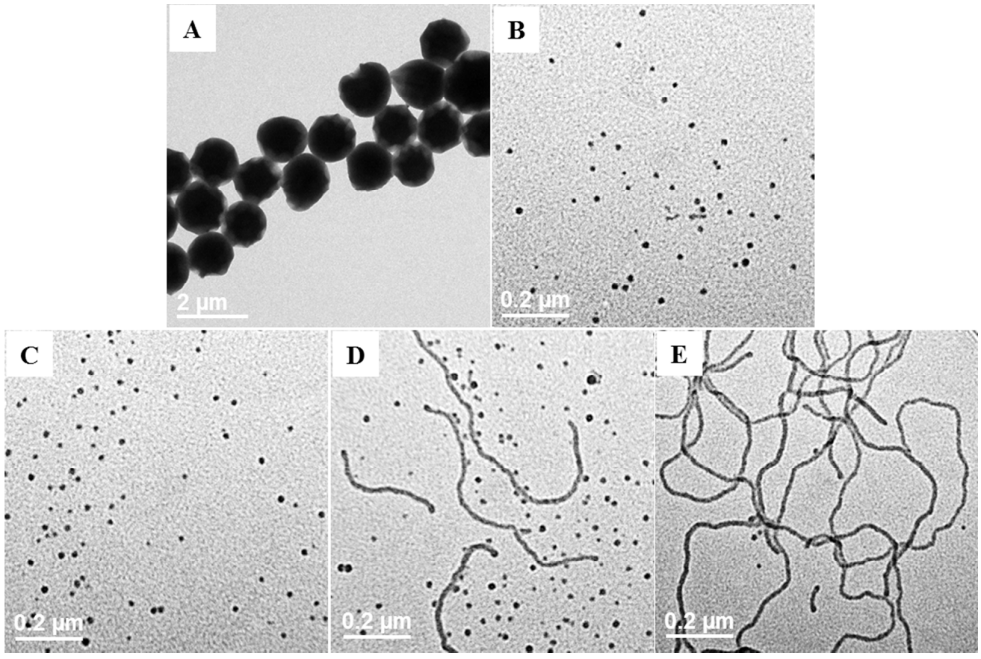

Figure 5. Representative TEM images of the latexes of diblock copolymer B3 in water after 4.5 h of polymerization, and after adding different amounts of toluene (A) 0 µL/mL, (B) 20 µL/mL, (C) 40 µL/mL, (D) 80 µL/mL, (E) 160 µL/mL, and then cooling to room temperature (23 ° C) for 24 h.

Conclusion

Five well-defined thermoresponsive copolymers based on DEGMA and HPMA components were successfully synthesized by RAFT-mediated solution polymerizations. The cloud point temperature of these copolymers could be predictably tuned by changing the HPMA content. The P($DEGMA_{29}$-co-$HPMA_6$)-$SC(=S)SC_2H_5$ is low-toxicity and suitable for the RAFT-mediated emulsion polymerization of styrene. By regulating the amount of plasticizer and feed ratio of styrene to macro-CTA, nanoaggregates with tunable morphologies were successfully produced in water. The ability to produce nanoaggregates from low-toxicity materials with both spherical and non-spherical shape will enable further fundamental studies of morphological effects on the interactions between nanoparticles and biological systems. Moreover, these novel nanoparticles have high potential as a platform for the next generation of nanotherapeutics with improved clinical outcomes.

Acknowledgements

This work was carried out within the Australian Research Council (ARC) Centre of Excellence in Convergent Bio-Nano Science and Technology (Project No. CE140100036). T.P.D. is grateful for the award of an Australian Laureate Fellowship from the ARC. N.P.T. acknowledges the financial support from the Faculty of Pharmacy and Pharmaceutical Sciences, Monash University.

References

(1) Cheng, C. J.; Tietjen, G. T.; Saucier-Sawyer, J. K.; Saltzman, W. M. *Nat. Rev. Drug Discovery* **2015**, *14*, 239.
(2) Veiseh, O.; Tang, B. C.; Whitehead, K. A.; Anderson, D. G.; Langer, R. *Nat. Rev. Drug Discovery* **2015**, *14*, 45.
(3) Brinkhuis, R. P.; Rutjes, F. P. J. T.; van Hest, J. C. M. *Polym Chem-Uk* **2011**, *2*, 1449.
(4) Lasic, D. D.; Papahadjopoulos, D. *Science* **1995**, *267*, 1275.
(5) Lammers, T.; Kiessling, F.; Hennink, W. E.; Storm, G. *J. Controlled Release* **2012**, *161*, 175.

(6) Mitragotri, S.; Anderson, D. G.; Chen, X.; Chow, E. K.; Ho, D.; Kabanov, A. V.; Karp, J. M.; Kataoka, K.; Mirkin, C. A.; Petrosko, S. H.; Shi, J.; Stevens, M. M.; Sun, S.; Teoh, S.; Venkatraman, S. S.; Xia, Y.; Wang, S.; Gu, Z.; Xu, C. *ACS Nano* **2015**, *9*, 6644.
(7) Howes, P. D.; Chandrawati, R.; Stevens, M. M. *Science* **2014**, *346*, 53.
(8) Truong, N. P.; Gu, W. Y.; Prasadam, I.; Jia, Z. F.; Crawford, R.; Xiao, Y.; Monteiro, M. J. *Nat. Commun.* **2013**, *4*.
(9) Schutz, C. A.; Juillerat-Jeanneret, L.; Mueller, H.; Lynch, I.; Riediker, M.; Consortium, N. *Nanomed.* **2013**, *8*, 449.
(10) Lytton-Jean, A. K.; Kauffman, K. J.; Kaczmarek, J. C.; Langer, R. *Cancer Treat. Res.* **2015**, *166*, 293.
(11) Etheridge, M. L.; Campbell, S. A.; Erdman, A. G.; Haynes, C. L.; Wolf, S. M.; McCullough, J. *Nanomed-Nanotechnol* **2013**, *9*, 1.
(12) Bae, Y. H.; Park, K. *J. Controlled Release* **2011**, *153*, 198.
(13) Park, K. *ACS Nano* **2013**, *7*, 7442.
(14) Daum, N.; Tscheka, C.; Neumeyer, A.; Schneider, M. *Wiley Interdiscip. Rev. Nanomed. Nanobiotechnol.* **2012**, *4*, 52.
(15) Toy, R.; Peiris, P. M.; Ghaghada, K. B.; Karathanasis, E. *Nanomed.* **2014**, *9*, 121.
(16) Truong, N. P.; Quinn, J. F.; Dussert, M. V.; Sousa, N. B. T.; Whittaker, M. R.; Davis, T. P. *ACS Macro Letters* **2015**, *4*, 381.
(17) Caldorera-Moore, M.; Guimard, N.; Shi, L.; Roy, K. *Expert Opin. Drug Deliv.* **2010**, *7*, 479.
(18) Truong, N. P.; Whittaker, M. R.; Mak, C. W.; Davis, T. P. *Expert Opin. Drug Deliv.* **2015**, *12*, 129.
(19) Geng, Y.; Dalhaimer, P.; Cai, S.; Tsai, R.; Tewari, M.; Minko, T.; Discher, D. E. *Nat. Nanotechnol.* **2007**, *2*, 249.
(20) Vivo, B.; Huang, X.; Li, L.; Liu, T.; Hao, N.; Liu, H.; Chen, D.; Tang, F. *ACS Nano* **2011**, *5*, 5390.
(21) Hu, X. L.; Hu, J. M.; Tian, J.; Ge, Z. S.; Zhang, G. Y.; Luo, K. F.; Liu, S. Y. *J. Am. Chem. Soc.* **2013**, *135*, 17617.
(22) Christian, D. A.; Cai, S.; Garbuzenko, O. B.; Harada, T.; Allison, L.; Minko, T.; Discher, D. E. *Mol. Pharm.* **2009**, *6*, 1343.
(23) Barua, S.; Yoo, J. W.; Kolhar, P.; Wakankar, A.; Gokarn, Y. R.; Mitragotri, S. *Proc. Natl. Acad. Sci. U. S. A.* **2013**, *110*, 3270.
(24) Karagoz, B.; Esser, L.; Duong, H. T.; Basuki, J. S.; Boyer, C.; Davis, T. P. *Polym Chem-Uk* **2014**, *5*, 350.
(25) Kolhar, P.; Doshi, N.; Mitragotri, S. *Small* **2011**, *7*, 2094.
(26) Barua, S.; Mitragotri, S. *ACS Nano* **2013**, *7*, 9558.
(27) Zhang, K.; Fang, H.; Chen, Z.; Taylor, J.-S. a.; Wooley, K. L. *Bioconjugate Chem.* **2008**, *19*, 1880.
(28) Florez, L.; Herrmann, C.; Cramer, J. M.; Hauser, C. P.; Koynov, K.; Landfester, K.; Crespy, D.; Mailander, V. *Small* **2012**, *8*, 2222.
(29) Zhang, Y.; Tekobo, S.; Tu, Y.; Zhou, Q. F.; Jin, X. L.; Dergunov, S. A.; Pinkhassik, E.; Yan, B. *ACS Appl. Mater. Interfaces* **2012**, *4*, 4099.
(30) Paul, D.; Achouri, S.; Yoon, Y. Z.; Herre, J.; Bryant, C. E.; Cicuta, P. *Biophys. J.* **2013**, *105*, 1143.
(31) Smith, A. E.; Xu, X. W.; Mccormick, C. L. *Prog. Polym. Sci.* **2010**, *35*, 45.
(32) Roy, D.; Brooks, W. L. A.; Sumerlin, B. S. *Chem. Soc. Rev.* **2013**, *42*, 7214.
(33) Talelli, M.; Hennink, W. E. *Nanomed.* **2011**, *6*, 1245.
(34) Convertine, A. J.; Lokitz, B. S.; Vasileva, Y.; Myrick, L. J.; Scales, C. W.; Lowe, A. B.; McCormick, C. L. *Macromolecules* **2006**, *39*, 1724.
(35) McKee, J. R.; Ladmiral, V.; Niskanen, J.; Tenhu, H.; Armes, S. P. *Macromolecules* **2011**, *44*, 7692.
(36) Sundararaman, A.; Stephan, T.; Grubbs, R. B. *J. Am. Chem. Soc.* **2008**, *130*, 12264.

(37) Moughton, A. O.; Patterson, J. P.; O'Reilly, R. K. *Chem. Commun.* **2011**, *47*, 355.
(38) Moughton, A. O.; O'Reilly, R. K. *Chem. Commun.* **2010**, *46*, 1091.
(39) Cai, Y.; Aubrecht, K. B.; Grubbs, R. B. *J. Am. Chem. Soc.* **2011**, *133*, 1058.
(40) Ke, X. X.; Wang, L.; Xu, J. T.; Du, B. Y.; Tu, Y. F.; Fan, Z. Q. *Soft Matter* **2014**, *10*, 5201.
(41) Qian, J.; Wu, F. P. *Macromolecules* **2008**, *41*, 8921.
(42) Jia, Z. F.; Bobrin, V. A.; Truong, N. P.; Gillard, M.; Monteiro, M. J. *J. Am. Chem. Soc.* **2014**, *136*, 5824.
(43) Qiu, X. P.; Tanaka, F.; Winnik, F. M. *Macromolecules* **2007**, *40*, 7069.
(44) Vihola, H.; Laukkanen, A.; Valtola, L.; Tenhu, H.; Hirvonen, J. *Biomaterials* **2005**, *26*, 3055.
(45) Harsh, D. C.; Gehrke, S. H. *J. Controlled Release* **1991**, *17*, 175.
(46) Lavigueur, C.; Garcia, J. G.; Hendriks, L.; Hoogenboom, R.; Cornelissen, J. J. L. M.; Nolte, R. J. M. *Polym Chem-Uk* **2011**, *2*, 333.
(47) Lynch, I.; Salvati, A.; Dawson, K. A. *Nat. Nanotechnol.* **2009**, *4*, 546.
(48) Congdon, T.; Shaw, P.; Gibson, M. I. *Polym Chem-Uk* **2015**, *6*, 4749.
(49) Chua, G. B. H.; Roth, P. J.; Duong, H. T. T.; Davis, T. P.; Lowe, A. B. *Macromolecules* **2012**, *45*, 1362.
(50) Lutz, J. F. *J. Polym. Sci., Part A: Polym. Chem.* **2008**, *46*, 3459.
(51) Hu, Z. B.; Cai, T.; Chi, C. L. *Soft Matter* **2010**, *6*, 2115.
(52) Vancoillie, G.; Frank, D.; Hoogenboom, R. *Prog. Polym. Sci.* **2014**, *39*, 1074.
(53) Lutz, J. F.; Hoth, A. *Macromolecules* **2006**, *39*, 893.
(54) Lutz, J. F.; Akdemir, O.; Hoth, A. *J. Am. Chem. Soc.* **2006**, *128*, 13046.
(55) Han, S.; Hagiwara, M.; Ishizone, T. *Macromolecules* **2003**, *36*, 8312.
(56) Jonas, A. M.; Glinel, K.; Oren, R.; Nysten, B.; Huck, W. T. S. *Macromolecules* **2007**, *40*, 4403.
(57) Luzon, M.; Boyer, C.; Peinado, C.; Corrales, T.; Whittaker, M.; Tao, L.; Davis, T. P. *J. Polym. Sci., Part A: Polym. Chem.* **2010**, *48*, 2783.
(58) Lutz, J. F.; Weichenhan, K.; Akdemir, O.; Hoth, A. *Macromolecules* **2007**, *40*, 2503.
(59) Shen, W. Q.; Chang, Y. L.; Liu, G. Y.; Wang, H. F.; Cao, A. N.; An, Z. S. *Macromolecules* **2011**, *44*, 2524.
(60) Khine, Y. Y.; Jiang, Y.; Dag, A.; Lu, H.; Stenzel, M. H. *Macromol. Biosci.* **2015**, *15*, 1091.
(61) Lutz, J. F.; Andrieu, J.; Uzgun, S.; Rudolph, C.; Agarwal, S. *Macromolecules* **2007**, *40*, 8540.
(62) Zengin, A.; Yildirim, E.; Caykara, T. *J. Polym. Sci., Part A: Polym. Chem.* **2013**, *51*, 954.
(63) Wischerhoff, E.; Uhlig, K.; Lankenau, A.; Borner, H. G.; Laschewsky, A.; Duschl, C.; Lutz, J. F. *Angew. Chem. Int. Edit.* **2008**, *47*, 5666.
(64) Truong, N. P.; Dussert, M. V.; Whittaker, M. R.; Quinn, J. F.; Davis, T. P. *Polym Chem-Uk* **2015**, *6*, 3865.
(65) Plummer, R.; Hill, D. J. T.; Whittaker, A. K. *Macromolecules* **2006**, *39*, 8379.
(66) Yu, B.; Chan, J. W.; Hoyle, C. E.; Lowe, A. B. *J. Polym. Sci., Part A: Polym. Chem.* **2009**, *47*, 3544.
(67) Tran, N. T. D.; Truong, N. P.; Gu, W. Y.; Jia, Z. F.; Cooper, M. A.; Monteiro, M. J. *Biomacromolecules* **2013**, *14*, 495.
(68) Nuhn, L.; Barz, M.; Zentel, R. *Macromol. Biosci.* **2014**, *14*, 607.
(69) Tucker, B. S.; Sumerlin, B. S. *Polym Chem-Uk* **2014**, *5*, 1566.
(70) Wutzel, H.; Richter, F. H.; Li, Y.; Sheiko, S. S.; Klok, H. A. *Polym Chem-Uk* **2014**, *5*, 1711.
(71) Chang, C. W.; Bays, E.; Tao, L.; Alconcel, S. N. S.; Maynard, H. D. *Chem. Commun.* **2009**, 3580.
(72) Pissuwan, D.; Boyer, C.; Gunasekaran, K.; Davis, T. P.; Bulmus, V. *Biomacromolecules* **2010**, *11*, 412.
(73) Shi, Y.; van den Dungen, E. T. A.; Klumperman, B.; van Nostrum, C. F.; Hennink, W. E. *Acs Macro Letters* **2013**, *2*, 403.

(74) Tasaki, K. *J. Am. Chem. Soc.* **1996**, *118*, 8459.
(75) Israelachvili, J. *Proc. Natl. Acad. Sci. U. S. A.* **1997**, *94*, 8378.
(76) Chee, C. K.; Hunt, B. J.; Rimmer, S.; Rutkaite, R.; Soutar, I.; Swanson, L. *Soft Matter* **2009**, *5*, 3701.
(77) De, P.; Sumerlin, B. S. *Macromol. Chem. Phys.* **2013**, *214*, 272.
(78) Ward, M. A.; Georgiou, T. K. *Polymers-Basel* **2011**, *3*, 1215.
(79) Griffiths, P. C.; Hirst, N.; Paul, A.; King, S. M.; Heenan, R. K.; Farley, R. *Langmuir* **2004**, *20*, 6904.
(80) Walter, R.; Ricka, J.; Quellet, C.; Nyffenegger, R.; Binkert, T. *Macromolecules* **1996**, *29*, 4019.
(81) Jia, Z. F.; Truong, N. P.; Monteiro, M. J. *Polym Chem-Uk* **2013**, *4*, 233.
(82) Cai, T.; Marquez, M.; Hu, Z. B. *Langmuir* **2007**, *23*, 8663.
(83) Lynd, N. A.; Meuler, A. J.; Hillmyer, M. A. *Prog. Polym. Sci.* **2008**, *33*, 875.
(84) Pietsch, C.; Mansfeld, U.; Guerrero-Sanchez, C.; Hoeppener, S.; Vollrath, A.; Wagner, M.; Hoogenboom, R.; Saubern, S.; Thang, S. H.; Becer, C. R.; Chiefari, J.; Schubert, U. S. *Macromolecules* **2012**, *45*, 9292.
(85) Barton, A. F. M. *Chem. Rev.* **1975**, *75*, 731.
(86) Mai, Y.; Eisenberg, A. *Chem. Soc. Rev.* **2012**, *41*, 5969.
(87) Cameron, N. S.; Corbierre, M. K.; Eisenberg, A. *Can. J. Chem.* **1999**, *77*, 1311.
(88) Warren, N. J.; Armes, S. P. *J. Am. Chem. Soc.* **2014**, *136*, 10174.
(89) Figg, C. A.; Simula, A.; Gebre, K. A.; Tucker, B. S.; Haddleton, D. M.; Sumerlin, B. S. *Chem Sci* **2015**, *6*, 1230.
(90) Holder, S. J.; Sommerdijk, N. A. J. M. *Polym Chem-Uk* **2011**, *2*, 1018.
(91) Rieger, J. *Macromol. Rapid Commun.* **2015**, *36*, 1458.
(92) Guerin, G.; Wang, H.; Manners, I.; Winnik, M. A. *J. Am. Chem. Soc.* **2008**, *130*, 14763.
(93) Gan, Y. D.; Dong, D. H.; Hogenesch, T. E. *Macromolecules* **1995**, *28*, 383.
(94) Blanazs, A.; Verber, R.; Mykhaylyk, O. O.; Ryan, A. J.; Heath, J. Z.; Douglas, C. W. I.; Armes, S. P. *J. Am. Chem. Soc.* **2012**, *134*, 9741.

For Table of Contents Use Only

Facile Production of Nanoaggregates with Tuneable Morphologies From Thermoresponsive P(DEGMA-co-HPMA)

Nghia P. Truong,[a] Michael R. Whittaker,[a] Athina Anastasaki,[a,b] David M. Haddleton,[a,b] John F. Quinn*[a] and Thomas P. Davis*[a,b]

[a] *ARC Centre of Excellence in Convergent Bio-Nano Science & Technology, Monash Institute of Pharmaceutical Sciences, Monash University, Parkville, Melbourne, Victoria 3052, Australia.*

[b] *Department of Chemistry, University of Warwick, Coventry CV4 7AL, United Kingdom.*

RAFT-mediated emulsion polymerization of styrene and subsequent morphological transition produces nanoaggregates with tuneable morphologies.